INL/JOU-23-70741-Revision-0

Investigations into Plasma-Mediated Decomposition of Organoiodide Species as a Pretreatment for Mitigation of Radioiodine Emissions

January 2022

Chaithanya Balumuru, John Stanford, Krishnan Raja, Piyush Sabharwall, Vivek Utgikar

Changing the World's Energy Future

Idaho National Laboratory

INL is a U.S. Department of Energy National Laboratory operated by Battelle Energy Alliance, LLC

INL/JOU-23-70741-Revision-0

Investigations into Plasma-Mediated Decomposition of Organoiodide Species as a Pretreatment for Mitigation of Radioiodine Emissions

Chaithanya Balumuru, John Stanford, Krishnan Raja, Piyush Sabharwall, Vivek Utgikar

January 2022

Idaho National Laboratory
Idaho Falls, Idaho 83415

http://www.inl.gov

Prepared for the
U.S. Department of Energy
Under DOE Idaho Operations Office
Contract DE-AC07-05ID14517

Investigations into plasma-mediated decomposition of organoiodide species as a pretreatment for mitigation of radioiodine emissions

Chaithanya Balumuru[a], John Stanford[a], Krishnan Raja[a], Piyush Sabharwall[b], and Vivek Utgikar[a,*]

[a]*Department of Chemical and Biological Engineering, University of Idaho, Moscow, ID 83844, USA*
[b]*Idaho National Laboratory, Idaho Falls, ID 83415, USA*

GRAPHICAL ABSTRACT

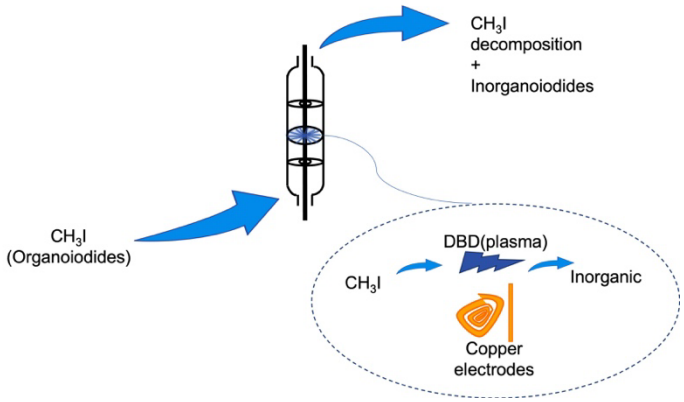

ABSTRACT

A plasma-mediated pretreatment step is proposed to decompose methyl iodide (CH_3I) for facilitating the capture of the iodine radioisotopes present in off-gas stream from used nuclear fuel reprocessing operations. Simulated CH_3I gas streams were exposed to dielectric barrier discharge (DBD) plasma in a quartz glass continuous flow reactor using copper electrodes. The kinetics of decomposition of CH_3I in nitrogen was investigated by varying the applied voltage, inlet concentration, and residence time. The rate of decomposition was proportional to CH_3I concentration and increased as the applied potential was increased. This effect was incorporated in the kinetics through the dependence of the rate constant on the applied electric field. Decomposition of CH_3I was not affected by moisture and the DBD pretreatment is likely to be as effective in the air environment as well, however, the results were confounded by a plasma-mediated reaction between nitrogen and oxygen.

Keywords

Methyl iodide
Organoiodide
Dielectric barrier discharge
Electric field
Decomposition
Reaction kinetics

[*]**Corresponding Author.**
E-mail address: *vutgikar@uidaho.edu (Dr. Vivek Utgikar)*

Nomenclature

Variables

$[A]$	Concentration (mol L^{-1})
C_1	Constant derived in terms of voltage
E_{avg}	Average electric field (kV m^{-1})
E	Electric Field (kV m^{-1})
k_0	Constant (s^{-1})
k	Rate Constant (s^{-1})
L	Length of the electrode (m)
n	Order of reaction
Q	Volumetric flowrate (L s^{-1})
R	Radius of inner electrode (m)
r_w	Radius between the inner electrode and the glass wall (m)
r	Radial distance (m)
$-r_A$	Reaction rate (mol m^{-3} s^{-1})
V	Volume of reactor (m^3)
V_{ap}	Applied Voltage (kV)
X_A	Conversion

Greek letters

τ	Residence time (milliseconds)
α	Constant derived from rate constants and electric fields (dimensionless)
λ	Linear charge density (C m^{-1})
ϵ_0	Permittivity constant (F m^{-1})

ABBREVIATIONS

AC	Alternate current
COG	Cell off gas
DBD	Dielectric barrier discharge
DC	Direct current
DF	Decontamination factor
DOE	Department of Energy
DOG	Dissolver off gas
GC-ECD	Gas chromatograph with electron capture detector
NTP	Non-thermal plasma
SOG	Shear off-gas
UHP	Ultra high purity
UNF	Used nuclear fuel
VOCs	Volatile organic compound's
VOG	Vessel off gas
WOG	Waste off gas

1. INTRODUCTION

Plasma is created when the constituents of a gas or liquid are transformed into ionized state upon addition of energy. Plasmas are well-known in industrial applications such as material processing, semiconductor fabrication, light sources, propulsion, and lasers, among others. The are also gaining interest in biology, environmental, and medicinal applications. Plasma can also be used to clean surfaces of various materials. Traditional solvent-based chemical treatments cannot activate or functionalize surfaces in the same manner as plasma does [1-4]. Plasma offers a wide range of applications due to the rapid chemical reactions that occur more selectively at lower temperatures or voltages than without plasma. Environmental applications of plasmas include air pollution treatment, wastewater and drinking water purification, and solid waste thermal disposal. An increasing number of investigations of plasma processes focus on the decomposition of nitrogen and sulfur oxides in flue gases, as well as volatile organic compounds (VOC) produced by various industrial processes.

In this study, we report on the environmental application of electric discharge plasma to decompose harmful methyl iodide (CH_3I) gas in an off-gas emission stream from a nuclear fuel reprocessing facility to increase the effectiveness of the subsequent capture of radioactive iodine (^{129}I) through adsorption. Nuclear energy generation, a non-carbon form of energy, is expected to rise in the next years, according to the Energy Information Administration of the U.S. DOE (Department of Energy) [5, 6]. Recycling uranium from the used nuclear fuel (UNF) will be necessary for both sustaining nuclear energy production over the long term in light of the scarcity of virgin uranium and reducing the volume of nuclear waste generated in the power plant operation. Off-gas streams from a UNF recycling facility's comprise of dissolver off-gas (DOG), vessel off-gas (VOG), cell off-gas (COG), waste off-gas (WOG), and the shear off-gas (SOG) that contain volatile radionuclides such as ^{129}I, ^{85}Kr, ^{3}H, and ^{14}C [7]. Improving the waste management from these facilities necessitates the capture and immobilization of radionuclides for the protection of human health and the environment, as well as ensuring regulatory compliance. Iodine has high mobility and tendency to bio-accumulate. Among these isotopes, ^{129}I has a very high half-life of more than 15 million years which requires special consideration [8,9]. The DOG and VOG streams emit the majority of radioiodine, with the VOG having iodine levels in parts per billion (ppb), with most of it present as organic iodides [10-12].

The chemical speciation of iodine has a significant impact on the most extensively used treatment approach – sorption capture [13]. It is far more difficult to remove organic iodide compounds through adsorption than it is to remove molecular iodine. Therefore, we propose decomposing the organic iodide to liberate molecular iodine from it prior to feeding the off-gas stream to an adsorption column to facilitate the capture of radioiodine from the off-gas stream [14-16]. This also paves the path for a more sustainable and greener nuclear energy production using spent uranium [6,17].

In this study the decomposition of organoiodide is achieved through the use of an electric discharge with active plasma in a dielectric barrier discharge (DBD) reactor. An active plasma is one in which an electrical discharge (or ionization) is maintained by an energy source such as direct current (DC) or alternating current (AC). For the generation of active plasma, it is also possible to

use a magnetic field or an electric field that changes with time [18]. A phenomenon known as electric discharge happens when an electric charge is transmitted across a gas medium between two electrical potential sites, which are formed as a result of the transmission of the charge [19,20]. Dielectric barrier discharge (DBD) is a nonequilibrium discharge created between two electrodes, at least one of which is covered by an insulator or a dielectric substance, such as glass or alumina, DBD plasma consists of excited species, free radicals, electrons, ions, and/or UV photons, which target a wide range of hazardous chemical compounds [21]. DBD is maintained by applying high AC voltages in the kV range and frequencies in the kHz range across the electrodes typically spaced a few millimeters apart [22]. As voltage is applied over the gap, charges accumulate along the surface of the insulator. Resulting local electric fields cause breakdown of material into ions and an avalanche of electrons from the cathode to the anode manifested as a thin, nearly cylindrical conductive filament [23].

DBD is a simple and effective method for producing electrons in a glass tube reactor with the inner and outer electrodes separated by the tube wall, as shown in the Fig. 1. Introducing plasma into a moving gas stream aids in the decomposition of organoidides (methyl iodide) existing in the stream. The typical voltage range used for this purpose is 2.5 kV to 5 kV. The current range used for this purpose is 1 mA to 30 mA. Controlling the intensity of the plasma can be accomplished by varying the applied voltage [24-26].

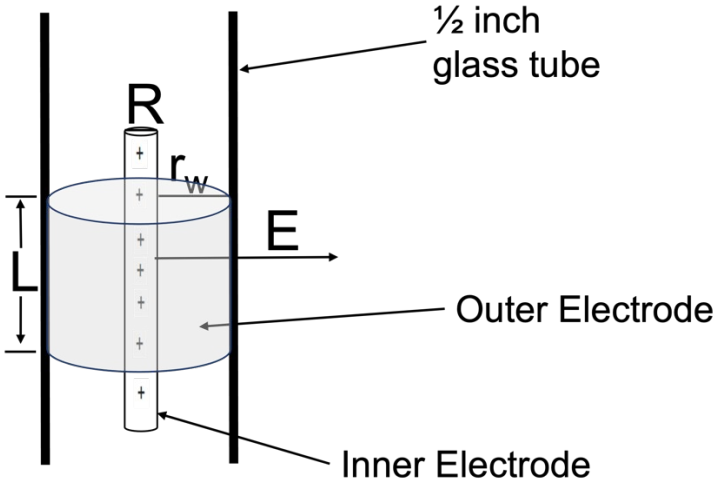

Fig. 1. Electric Field flow (L = Length of the outer electrode, R=Radius of inner electrode, r_w = Gap between the inner electrode and the glass wall, E = Electric Field)

In comparison to other types of electric discharge, such as pulsed corona, surface discharge, and gliding arc, DBD is considered to be more reliable. In a pulse corona discharge, high energy electrons are created, resulting in a short pulse regulated by a high voltage; pulsed corona is also referred to as temporary plasma activity [27]. Surface discharges can occur in a gas, liquid, or vacuum when they are adjacent to a solid dielectric surface [28]. Surface DBDs, on the other hand, are a sort of asymmetric dielectric barrier discharge (DBD) that can generate ions and cause aerodynamic forces in the air. The discharge happens in the gas above the dielectric surface, with both electrodes immersed in the insulator [29,30]. Energy efficiency, active flow control, and quick

reaction are all advantages of coplanar (surface discharge and surface DBD) discharges. Another type of discharge, the gliding arc, is characterized by rapid changes from high to low voltage levels with less stability in the plasma. DBD reactors are the most simple to operate and maintain since they can work at both low and high voltages and vastly used for gas streams. As a result, DBD is the most extensively utilized approach in non-thermal plasma generators [31-33].

In a gas, non-thermal plasma (NTP) is produced by electric discharge devices such as dielectric barrier discharge (DBD), corona discharge, gliding arc, and so forth. NTP is also referred to as low-temperature or cold plasma because to the fact that the temperature of the gas is lower than the temperature of the electrons in the plasma. NTP is also known as non-equilibrium plasma because there is thermodynamic disequilibrium between electrons and heavier particles. During the generation of plasma, electrons are produced first and they are accelerated in the electric field in a gas medium. NTP can also be produced at atmospheric or lower pressures [34-36]. It is typically described as a partially ionized gas containing a variety of charged and neutral particles. The type of discharge, physical parameters, and gas movement all have the potential to impact the plasma. Belasri et al. [37] study the production of non-thermal plasma at low pressures, using a computer model of homogeneous dielectric-barrier discharge in pure xenon over a wide frequency range of 50 kHz and gas pressures of 100–800 Torr. Wang et al. [38] used electrical and optical diagnosis, as well as temperature measurements, to illustrate the impacts of AC and ns pulse power supply on the discharge characteristics of coaxial DBD in order to produce double layer DBD that generates atmospheric pressure plasma. Goldberg et al. [39] used an electric field four-wave mixing approach to produce high-pressure transient plasmas by delivering nanosecond pulse discharge and measuring the electric field in high-pressure transient plasmas with sub-nanosecond temporal resolution. Eriksson et al. [40] established a process and apparatus for generating [11C]methyl iodide (CH_3I)from [11C]methane and iodine in an NTP reactor in a single pass and applied high voltage (400 V/31 kHz) to electrodes in a stream of helium gas at reduced pressure to generate the glow discharge plasma. This work by Eriksson et al. [40] is supported by Steacie and McDonald. [41], who proved that a reversible reaction of methyl iodide (CH_3I) occurs during thermal decomposition of methyl iodide (CH_3I) at various temperatures.

Steacie and McDonald. [41] demonstrated the kinetics of thermal decomposition of methyl iodide (CH_3I) at various temperatures, emphasizing the stability of methyl iodide (CH_3I) by reverse reaction. Ogg [42] provides detailed information on kinetic studies and the stability of methyl iodide (CH_3I) by reverse reaction, as well as kinetics studies for various alkali iodides with hydrogen iodide such as reaction rate and the rate constant in terms of temperature ranging from 250°C to 300°C and reactants pressures ranging from 50-100 mm. However, these pressure and temperature conditions are significantly different from those encountered in the vent off-gas (VOG) streams, necessitating application of electric discharge for decomposition at ambient temperatures and pressures. According to Mikheev et al. [43], atomic iodine concentrations produced by the decomposition of methyl iodide (CH_3I) by the products of a direct current glow discharge in an oxygen flow under pressured conditions with the active medium of an oxygen-iodine laser were determined. This study was largely concerned with reactions between iodine and oxygen, and it lacked information on reaction kinetics.

In our investigations, a continuous flow reactor was designed and operated with uniform plasma generated using DBD. CH_3I decomposition experiments were conducted under conditions similar to VOG streams as well as in nitrogen environments for broader applications. Parameters varied

in the study included the concentration of CH_3I, the flow rate of the gases, the applied voltage, and the composition of the gas. A kinetic model was proposed to describe the dependence of the decomposition rate on CH_3I concentration and electric field, and the rate parameters determined from the experimental data. The effect of presence of moisture on the CH_3I decomposition was also investigated.

2. Material and methods

2.1. Experimental Setup

The experimental setup that was employed in the investigations is depicted in Fig. 2. A gas cylinder containing nitrogen-methyl iodide (CH_3I) (vendor: Airgas; methyl iodide (CH_3I) concentration 1 ppm) served as the source of the methyl iodide. All experiments were carried out using non-radioactive substitutes. The flow from this source cylinder was blended with the flow from another gas cylinder (Ultra High Purity (UHP) nitrogen/air) to manipulate the concentration of the methyl iodide (CH_3I) in the gas fed to the reactor. All of the gases were procured from Airgas. Controlling the flow rates of two gases (the source and the balance/diluting gas) was accomplished through the use of mass flow controllers (FC1 and FC2) in order to keep the concentration of methyl iodide (CH_3I) at a constant value. The reactor system was constructed using methyl iodide-resistant materials such as fluorinated ethylene propylene (FEP) and stainless steel (SS) tubing from Grainger, as well as nylon fittings from MacMaster. Initial investigations using borosilicate glass reactor revealed that reactor wall tended to develop pinholes leading to a collapse of the plasma. This necessitated a changeover to a quartz tube reactor which did not exhibit such tendency. The reactor setup was placed in a fume hood for safety. The quart tube wall separated the two copper electrodes – an inner electrode made of polished copper wire with a diameter of 0.5 mm is placed in the center with the help of fritted discs, and an outer electrode made of a 0.002 mm thick, 3 mm wide strip copper sheet wrapped on the outside of the quartz tube (both procured from Nextmetal). Copper was found to be more suitable than other materials such as tungsten because of its lower voltage requirement for a stable plasma. In the experiments, copper electrodes were charged using a NeonPro Company HB-11010 (10kV, 30mA) voltage source with an output voltage ranging from 1kV to 10kV and the voltage was adjusted using a Variac TDGC-2KVA variable voltage regulator. A mass flow meter from Teledyne Hastings-Raydist or bubble flow meter was used to measure the flow at the outlet. Outlet from the reactor is directed to the GC-ECD which control an internal electronic gas-sampling valve to take controlled volume samples with the help of peak simple software. All experiments were conducted at the ambient temperature of the laboratory, which is around 25°C, and atmospheric pressure.

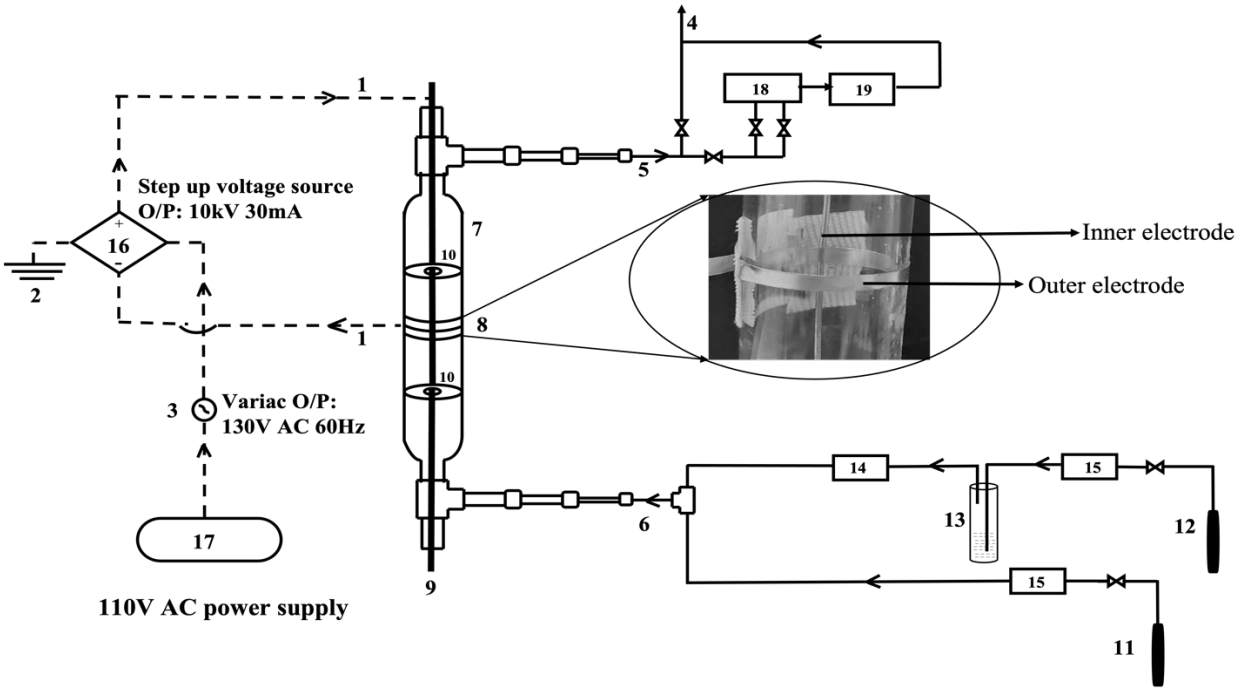

Fig. 2. Experimental setup

Numbers: 1. Electric Wire, 2. Ground, 3. AC Controller, 4. Vent, 5. Gas Outlet, 6. Gas Inlet, 7. Glass Tube, 8. Outer Electrode, 9. Inner Electrode, 10. Fritted Discs, 11. Diluting gases source, 12. CH_3I gas plus N_2 mixture source, 13. Humidifier, 14. Hygrometer, 15. Flow controller, 16. Voltage source, 17. Plug in, 18. Gas Chromatography, 19. Electron Capture Detector

2.2. Experimental Procedure

The methyl iodide (CH_3I) containing gas stream was passed through the continuous flow reactor. The accuracy of the flow controllers/meters and the absence of leakage from any piece of equipment in the setup was confirmed by measuring the flow rates of the outlet stream periodically using a bubble flow meter. Once the flow rate was established, plasma was generated in the reactor with the help of a voltage controller. The parameters varied in the experiments - the gas mixture, inlet methyl iodide (CH_3I) concentration, residence time, and applied voltage, are shown in the experimental matrix Table 1. Control experiments were conducted for each gas mixture wherein only the balance or diluent gas was subjected to electric discharge in absence of methyl iodide. All experiments were conducted in triplicate to ensure accuracy. The residence time is determined by the reactor volume, which is determined by the plasma volume.

Table 1
Experimental Matrix

Base case	CH_3I, N_2
Diluting Gases	N_2, Air

Concentration	150 ppb to 500 ppb
Residence Time	653 ms to 1176 ms
Voltage	3 kV to 5 kV

The outer and inner electrodes were changed at regular intervals after some time depending on their oxidizing status. Because of the exposure to air, the outer electrode had to be changed more frequently, approximately every three runs as illustrated in Fig. 3

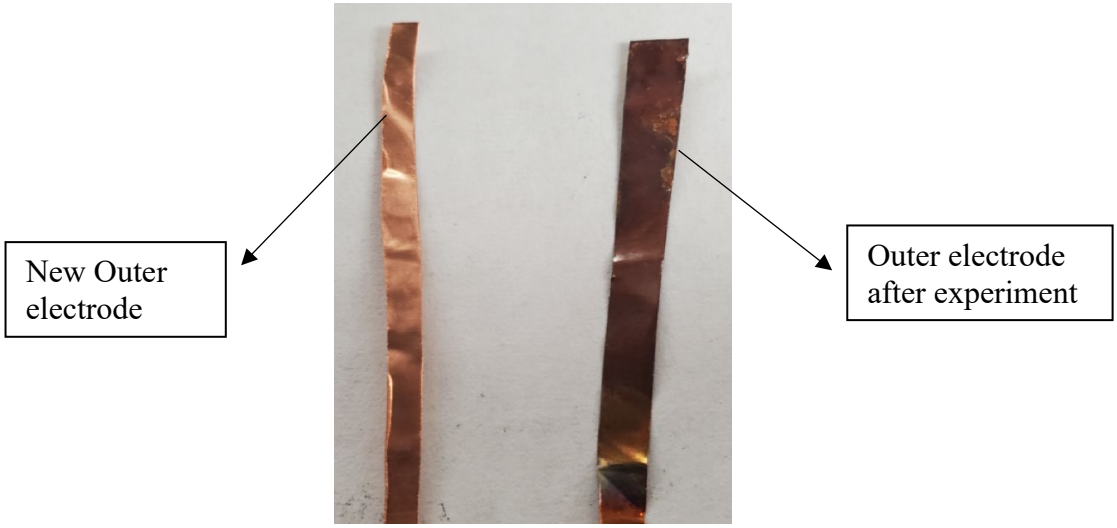

Fig. 3. Electrode comparison before and after experiments

2.3. Calibration and method of measurement

Gas chromatograph (SRI 8610C GC) with electron capture detector (GC-ECD) using a 6ft Restek Hayesep Q 1/8" OD packed column was used for quantitatively analyzing the methyl iodide (CH_3I) concentration. Exceptionally low concentrations up to 1ppb level of methyl iodide (CH_3I) can be detected by GC-ECD because of its extremely sensitive towards electronegative species. The experimental setup allowed the flow from reactor to be directed through the GC for sampling and analysis. The carrier gas for analysis was ultra-high purity nitrogen with a column inlet pressure of 25 psig and a constant flow rate of 20 mL/min. The GC and electronic sample valve were both 150°C while the ECD was 250°C. The constant current was 300 pA. By using certified 1ppm methyl iodide (CH_3I) in a nitrogen gas cylinder, the GC-ECD was calibrated for methyl iodide (CH_3I) gas.

3. Results and Discussion

3.1. Experimental data

The data obtained from the experiments are presented below. All the data are confirmed by running experiments multiple times. Initially base case experiments were performed with inert gas nitrogen (N_2) and followed by VOG stream conditions where air as a diluting gas instead of nitrogen.

3.1.1. Control runs (only nitrogen)

The control runs involved adjusting the flow rate of nitrogen to 100 mL/min and then subjecting it to the DBD. The chromatograms of the outlet stream were essentially identical to those of the inlet stream indicating that the nitrogen was inert to the effect of DBD. The results indicate that nitrogen has no interaction with DBD and is an excellent choice as a diluting gas in the methyl iodide (CH_3I) [14]decomposition experiments.

3.1.2. Methyl iodide (CH_3I) runs with nitrogen as diluting gas

In the first series of experiments, the nitrogen-methyl iodide (CH_3I) mixture was blended with UHP nitrogen in a ratio 1:4 (ratio of flow rates). The total flow rate of the mixed stream was 125 mL/min. The gas stream was subjected to DBD at a voltage of 3.5 kV and outlet stream analyzed for methyl iodide (CH_3I) as described in section 2.3.

The observed inlet concentration of methyl iodide (CH_3I) was 223 ppb, with traces of air (oxygen and carbon dioxide) and water in the chromatogram. In contrast, the complete disappearance of methyl iodide (CH_3I) peak in the outlet stream indicated complete decomposition. However, no changes in the air and water peaks were observed because the incremental quantities of carbon dioxide and water generated by the decomposition and subsequent reaction with oxygen are too small to be detected by the GC.

In the subsequent series of tests, the applied voltage, initial methyl iodide (CH_3I) concentration, and the flow rate was varied as described in section 2.2 and the results are described in section 3.1.2.1 and 3.1.2.2.

3.1.2.1 Voltage Variation

The inlet concentration of methyl iodide (CH_3I) and total flow rate of the gas stream were maintained at 465 ± 10 ppb and 75 mL/min, respectively, in these series of experiments. The observed outlet concentrations and calculated conversions are shown in Table 2, with a graphical representation in Fig. 4.

Table 2
Voltage variations at constant inlet concentration 465±10 ppb and at a constant total flow rate of 75 mL/min

Voltage (kV)	Average outlet concentration (ppb)	Conversion (X_A)
3.5	114	0.75
4	102	0.78
4.5	98	0.79
5	93	0.80

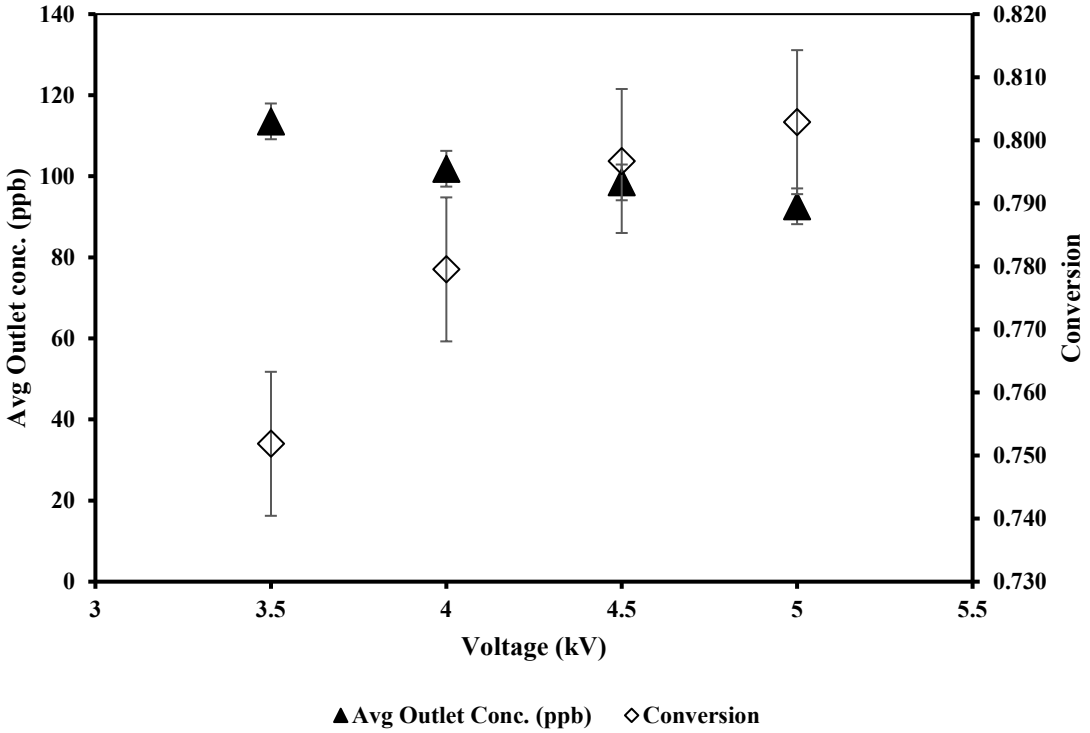

Fig. 4. Behavior of outlet concentration with a voltage variation

As shown in Table 2 and Fig. 4, the increase in voltage from 3.5 to 5 kV, the outlet concentration of methyl iodide (CH_3I) decreased from 114 ppb to 93 ppb, resulting in the highest conversion of 80 %. The reactor configuration could withstand stable plasma up to 5 kV of applied voltage. So, the concentration of methyl iodide (CH_3I) in the inlet was varied to demonstrate the ability of the DBD treatment to obtain complete destruction of the compound.

3.1.2.2. Concentration variation

The inlet concentration of methyl iodide (CH_3I) was varied by manipulating the ratio of the source and diluent gases. The total flow rate and applied voltage were maintained constant in these experiments at 75 mL/min and 3.5 kV, respectively. The details of these conditions, observed outlet concentrations, and calculated conversions are shown in Table 3 and represented graphically in Fig. 5 with obtained results.

Table 3
Results of concentration variations at constant applied voltage 3.5 kV and constant total flow rate of 75 mL/min

Source gas flow rate (mL/min)	Nitrogen gas flow rate (mL/min)	Inlet Concentration (ppb)	Average Outlet concentration (ppb)	Conversion (X_A)

50	25	501	108	0.78
40	35	468	107	0.77
25	50	399	83	0.79
15	60	303	51	0.83
10	65	242	29	0.88
5	70	150	10	0.94

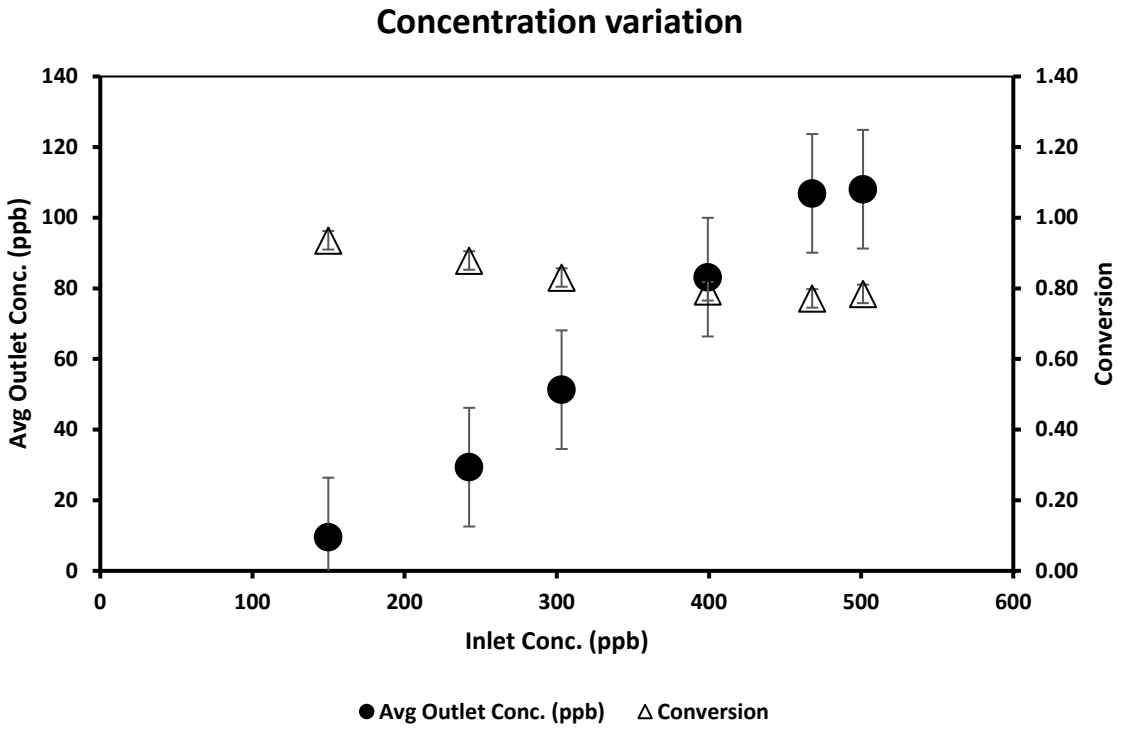

Fig. 5. Outlet concentration and conversion as function of inlet concentration at constant applied voltage 3.5 kV and constant total flow rate of 75 mL/min

The methyl iodide (CH_3I) concentration in the outlet stream increased from 10 ppb to 108 ppb when the inlet concentration was increased from 150 ppb to 500 ppb, as indicated in Table 3 and Fig. 5, resulting in a shift in conversion from 94 % to 78 %.

3.1.3. Control runs (only air)

The control runs with air, as in case of nitrogen, involved adjusting the flow rate of air in absence of methyl iodide (CH_3I) to 100 mL/min and then subjecting it to the DBD. The inlet sample is characterized by a large initial peak of air, followed by a small water peak. The outlet sample shows these peaks, as well as an extremely large peak appearing near the retention time of methyl iodide. The GC software identifies the compound as methyl iodide, even though, no methyl iodide (CH_3I) was present in the inlet stream.

3.1.4. Methyl iodide (CH_3I) runs with air as diluting gas

In the subsequent series of experiments, the reactor was fed with a gas stream obtained by blending 25 mL/min of 1 ppm methyl iodide (CH_3I) in nitrogen with 100 mL/min of air and subjected to DBD at a minimum voltage of 3.5 kV.

The observed inlet concentration of methyl iodide (CH_3I) was 236 ppb, with air (oxygen and carbon dioxide) peak and a small water peak. The outlet chromatogram shows several large, irregular peaks as. One of the peaks is identified as methyl iodide, though it is more likely to represent the products of the electric discharge driven reaction between oxygen and nitrogen. Similar results were obtained for other runs at different flow rates of air.

The experiments conducted with methyl iodide (CH_3I) in nitrogen environment demonstrated the effectiveness of electric discharge in decomposing methyl iodide. It is expected that similar destruction of methyl iodide (CH_3I) will occur in methyl iodide-air mixture. However, this destruction could not be confirmed due to confounding of results by formation of large quantities of unknown species, likely NO_x, that masked the ECD response to methyl iodide. The extremely high concentrations of oxygen and nitrogen compared to methyl iodide (CH_3I) (percentages as opposed to ppb levels) confound the analysis of methyl iodide. It is perhaps possible to develop an analytical technique that will allow one to discern the fate of methyl iodide (CH_3I) after treating the VOG by DBD. However, subjecting the VOG stream to DBD will also result in the formation of several undesired species including NO_x. These species, in turn, will hinder the capture of radioiodine species in the subsequent adsorption step in the treatment of off-gas emissions, as also create additional emission concerns.

These study results showed decomposition of low concentrations of methyl iodide (CH_3I) at the ppb level, which represents the concentration level of organoiodide in VOG stream. Kalinin et al. [44] observed methyl iodide (CH_3I) decomposition in their experiments conducted with air-methyl iodide (CH_3I) mixtures where methyl iodide (CH_3I) was present at significantly higher concentrations (150-3000 ppm). The decomposition was attributed to electric discharge, rather than homogeneous reaction between methyl iodide (CH_3I) and ozone generated through electric discharge.

No kinetic analysis was performed in these previous investigations. The data obtained from nitrogen-methyl iodide (CH_3I) mixture runs in the present study were analyzed to determine the kinetics of methyl iodide (CH_3I) decomposition under electric discharge as described in section 3.2.

3.2. Kinetic Model

Subjecting methyl iodide (CH_3I) to DBD likely results in its decomposition forming gaseous iodine [44], and hydrocarbon radicals, possibly as indicated by reaction R1, which is similar to that mentioned by Steacie and McDonald, and Ogg [41,42].

$$2CH_3I \xrightarrow{e-} CH_3 \cdot + I_2 \qquad \text{R1}$$

It is postulated that the hydrocarbon radicals will undergo further oxidation to carbon dioxide and water, however, the incremental quantities produced are too small to be detected in these experiments. DBD-mediated methyl iodide decomposition runs were also conducted in oxygen environment. The methyl iodide-nitrogen mixture was used as the source of methyl iodide, and hence nitrogen was also present in these experiments. The control runs with oxygen (DBD in absence of methyl iodide-nitrogen) reveal two peaks in the chromatogram – oxygen and ozone. Two additional peaks, attributed to water and NO_x, appear in the runs conducted with the presence of methyl iodide-nitrogen. The likely reaction is shown below in scheme R2, as suggested by Kalinin et al [44]. The carbon dioxide peak is not visible in the chromatogram, as it appears at the same retention time as oxygen, and the incremental amount formed is too insignificant to affect the original oxygen peak.

$$6CH_3I + 7O_3 \rightarrow 3I_2 + 6CO_2 + 9H_2O \qquad \text{R2}$$

The presumed product in the nitrogen environment, that is, in absence of oxygen, is ethane resulting from the combination of two methyl radicals, as indicated in the study conducted by Holm [45].

The rate of decomposition of methyl iodide (CH_3I) was modeled from its concentration data. A power law model was used to describe the dependence of the reaction rate on methyl iodide (CH_3I) concentration. The effect of electric discharge was incorporated in the rate equation by assuming the rate constant to be an Arrhenius equation function of the applied electric field. These power law rate expression in terms of concentration is described by Eq. (1) and Arrhenius equation which describing the mathematical relationship between applied electric field and rate of chemical reaction is described in Eq. (2).

$$-r_A = k_0 E^{\alpha} [A]^n \qquad (1)$$

where $-r_A$ is the rate of disappearance of methyl iodide, $[A]$ its concentration, and n the order of the reaction. The rate constant k is a function of the applied electric field E by using Arrhenius equation.

$$k = k_0 e^{\alpha E} \qquad (2)$$

The experimental concentration and flow rate data were used to obtain the rate of reaction as shown in Eq. (3). Q is the flow rate, $[A]_{in}$ and $[A]_{out}$ are the inlet and outlet concentrations of methyl iodide (CH_3I) and V is the volume of the reactor.

$$-r_A = \frac{Q([A]_{in} - [A]_{out})}{V} \qquad (3)$$

The values of rate constant at various applied electric fields were obtained by linearizing the rate equation as shown in Eq. (4) and performing linear regression of the experimental data. The constant k_0 and index α were obtain by similar linear regression of Eq. (2) as shown by Eq. (5).

$$\ln(-r_A) = n(\ln[A]) + lnk \tag{4}$$

$$lnk = \alpha E + lnk_0 \tag{5}$$

The electric field is a function of radial distance for the particular arrangement (one electrode at the center of a cylinder (glass tube), other electrode at a distance equal to the radius of the tube) as shown in Eq. (6): [46-49].

$$E = \frac{\lambda}{2\pi\epsilon_0 r} \tag{6}$$

where λ which is the charge density per unit length of the axial electrode, ϵ_0 is Permittivity constant of the medium, and r is the radial distance. The constants in the Eq. (6) were lumped together as shown in Eq. (7). An average electric field derived in terms of volume was used in the kinetic analysis, calculated as shown in Eq. (8), where the integration is carried out from the surface of the inner electrode (equal to its radius) to the inner radius of the reactor tube.

$$C_1 = \frac{\lambda}{2\pi\epsilon_0} \tag{7}$$

$$E_{avg} = \frac{\int E dV}{\int dV} \tag{8}$$

The value of constant C_1 was obtained from applied voltage as shown in Eq. (9) [46-49].

$$V_{ap} = \int_R^{r_w} E \cdot dr \tag{9}$$

Fig. 6 show the Eq. (4) plotted for the three different applied voltages of 3.5 kV, 4 kV, and 4.5 kV, respectively.

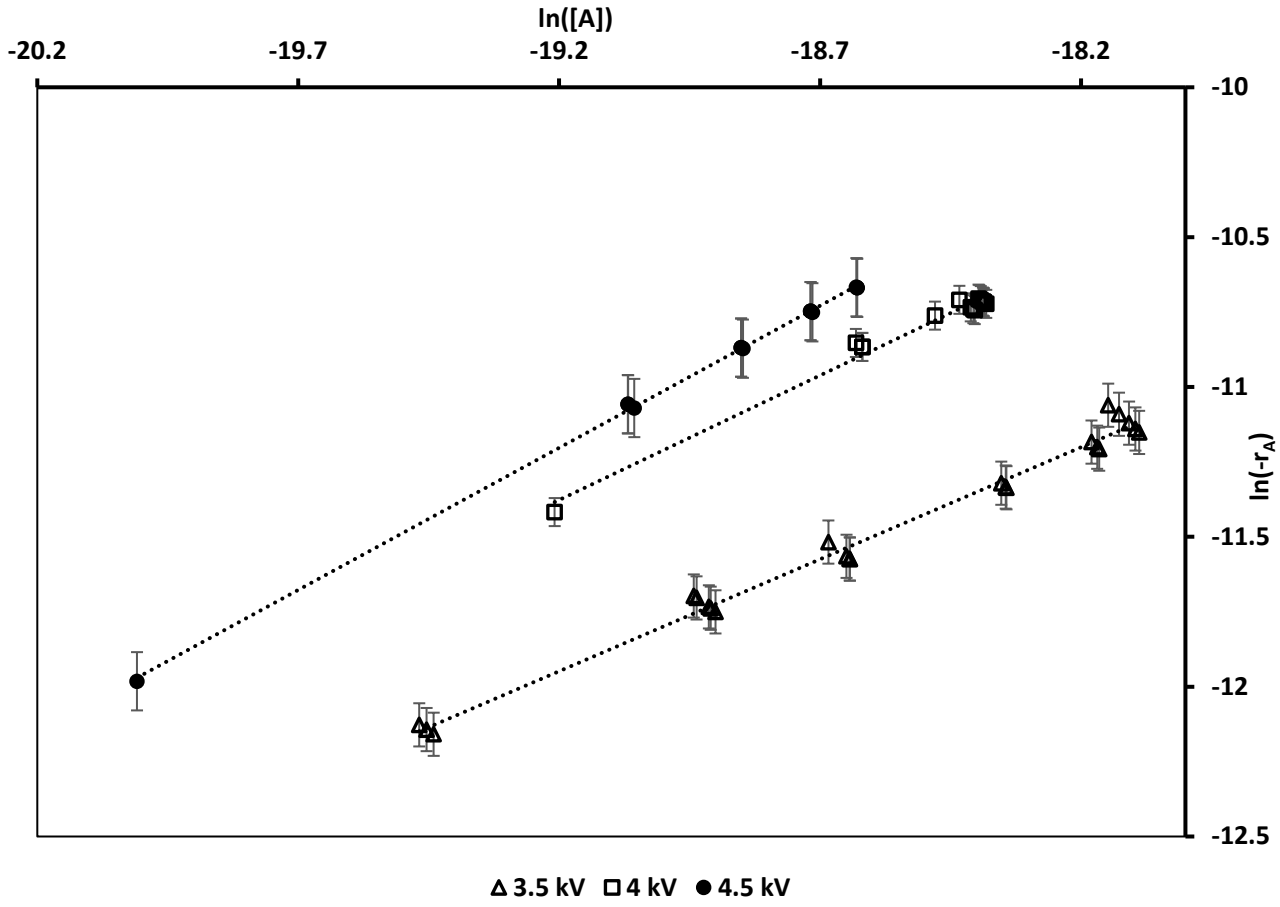

Fig. 6. ln(-r_A) vs ln(*[A]*) at applied voltages 3.5kV, 4kV, and 4.5 kV

Table 4
Results of rate constant and linear regression with correlation coefficient at different applied voltage from Fig. 6.

Voltage (kV)	ln(k)	Linear Regression equation	Correlation coefficient (R^2)
3.5	2.4014	y = 0.7474x + 2.4014	0.9801
4	4.5878	y = 0.8315x + 4.5878	0.9801
4.5	7.007	y = 0.9484x + 7.007	0.9992

Specifically, the intercepts in the fitted equation indicate the rate constants at different applied voltages, whereas, as shown in Table 4, the slope represents order of reaction in the system. As a first approximation, the reaction can be said of as being first order [41,42] with respect to the concentration of methyl iodide (CH_3I). Using Eq. (5), it is possible to investigate further the dependency of the rate constants on the electric field, as illustrated in Fig. 7.

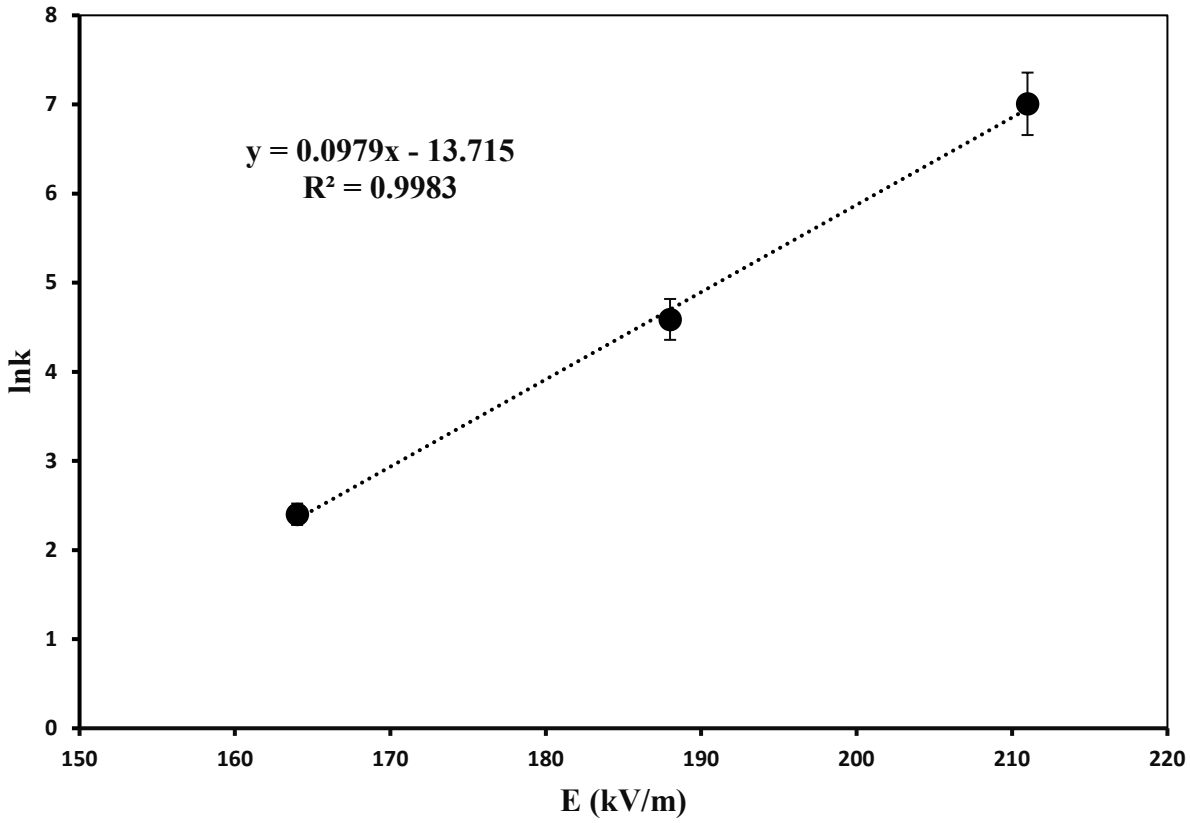

Fig. 7. Obtained constants with their applied electric field

From, Fig. 7 the high value of correlation coefficient (R^2) shows an excellent fit. The value of constant k_0 is 1.1057×10^{-6} s^{-1} and α is 0.0979.

The proposed model equation for methyl iodide (CH_3I) decomposition for voltage ranging from 3.5kV to 4.5kV can be written as Eq. (10).

$$-r_A = 1.1057 \times 10^{-6} \cdot e^{0.0979 \times E} \times [A] \quad \text{ppb/s} \tag{10}$$

Where the concentration *[A]* is expressed in ppb and *E* is the electric field in kV/m (kilo volt/meter).

3.3. Impact of moisture

The off-gases (DOG, VOG, etc.) from an aqueous reprocessing plants will typically contain high levels of moisture [12]. Whether the moisture impacts the DBD-mediated decomposition was examined by introducing humidity in the inlet gas stream. This was accomplished by sparging the balance/diluent nitrogen gas through a bubbler before blending it with the source methyl iodide-nitrogen stream as shown in Fig. 2. The relative humidity of the balance stream was 100% saturated as measured by a Fischer Scientific Traceable Hygrometer. The source stream is then mixed with the balance stream. The ratios of the balance and source streams were changed to get different

relative humidity values. The large peak at the water area in the chromatogram reflects the presence of moisture in the inlet stream. The decomposition of methyl iodide (CH_3I) can be seen in the chromatograms of the outlet sample. Methyl iodide (CH_3I) conversions in presence of moisture at various inlet concentrations are shown in Table 5. These conversions are only marginally lower (~1-2%) than those in absence of humidity, indicating that the presence of moisture had minor to no impact on the DBD process.

Table 5
Methyl iodide (CH_3I) decomposition in the presence of moisture.

Nitrogen flow rate (mL/min)	Source gas flow rate (mL/min)	Humidity (%)	Voltage (kV)	Inlet (ppb)	Outlet (ppb)	Conversion (X_A)
60	15	80	3.5 - 4.0	208	30	0.85
65	10	86	3.5 - 4.0	135	16	0.88
70	5	93	3.5 - 5.0	60	4	0.93

4. CONCLUSIONS

An experimental setup for producing dielectric non-thermal plasma was successfully developed. Quantitative decomposition of methyl iodide (CH_3I) in nitrogen environment was demonstrated for the DBD process. The kinetics of decomposition was modeled using power-law model, and Arrhenius equation, values of the kinetic parameter as well as their dependence on the applied electric field is determined. The presence of moisture did not affect the decomposition of methyl iodide (CH_3I) by DBD. It is expected that similar decomposition of methyl iodide (CH_3I) will occur if VOG stream were treated with DBD. However, this could not be confirmed in the experimentation conducted when air was blended with the methyl iodide-nitrogen source stream.

It is apparent that even though the objective of methyl iodide (CH_3I) decomposition was successfully accomplished through the application of DBD, this pretreatment technique is not a promising option for improving the management of organic radioiodine species from the UNF off-gas streams, due to electric discharge mediated reactions between oxygen and nitrogen present in the streams.

Declaration of Competing Interest

The authors declare that they have no known competing financial interests or personal relationships that could have appeared to influence the work reported in this paper.

ACKNOWLEDGEMENT

This research was supported through funding obtained from Department of Energy, Office of Nuclear Energy's Nuclear Energy University Program. [Project ID: DE-NE0008778, Project # 18-14998]

References

(1) Yang, Y.; Cho, Y. I.; Fridman, A. *Plasma Discharge in Liquid: Water Treatment and Applications*; CRC Press, 2017.

(2) Bogaerts, A.; Neyts, E.; Gijbels, R.; Mullena, J. V. D. Review Gas Discharge Plasmas and Their Applications. *spectrochimica acta part b*. **2001**, *57*(4), 609–658.

(3) Kelar Tučeková, Z.; Vacek, L.; Krumpolec, R.; Kelar, J.; Zemánek, M.; Černák, M.; Růžička, F. Multi-Hollow Surface Dielectric Barrier Discharge for Bacterial Biofilm Decontamination. *Molecules.* **2021**, *26* (4), 910. https://doi.org/10.3390/molecules26040910.

(4) Hempel, F.; Steffen, H.; Busse, B.; Finke, B.; Nebe, J. B.; Quade, A.; Rebl, H.; Bergemann, C.; Weltmann, K.-D.; Schröder, K. On the Application of Gas Discharge Plasmas for the Immobilization of Bioactive Molecules for Biomedical and Bioengineering Applications; *Intech,* **2011**, 298-318. https://doi.org/10.5772/19043.

(5) International Energy Outlook - U.S. Energy Information Administration (EIA) https://www.eia.gov/outlooks/ieo/index.php (accessed 2021 -12 -11).

(6) Taebi, B.; Kloosterman, J. L. To Recycle or Not to Recycle? An Intergenerational Approach to Nuclear Fuel Cycles. *Sci Eng Ethics.* **2008**, *14* (2), 177–200. https://doi.org/10.1007/s11948-007-9049-y.

(7) Huve, J.; Ryzhikov, A.; Nouali, H.; Lalia, V.; Augé, G.; Daou, T. J. Porous Sorbents for the Capture of Radioactive Iodine Compounds: A Review. *RSC Adv.* **2018**, *8* (51), 29248–29273. https://doi.org/10.1039/C8RA04775H.

(8) Chapman, K. W.; Chupas, P. J.; Nenoff, T. M. Radioactive Iodine Capture in Silver-Containing Mordenites through Nanoscale Silver Iodide Formation. *J. Am. Chem. Soc.* **2010**, *132* (26), 8897–8899. https://doi.org/10.1021/ja103110y.

(9) Nandanwar, S. U.; Dantas, J.; Coldsnow, K.; Green, M.; Utgikar, V.; Sabharwall, P.; Aston, D. E. Porous Microsphere of Magnesium Oxide as an Effective Sorbent for Removal of Volatile Iodine from Off-Gas Stream. *Adsorption.* **2016**, *22* (3), 335–345. https://doi.org/10.1007/s10450-016-9781-1.

(10) Jubin, R. T.; Strachan, D. M.; Soelberg, N. R. *Iodine Pathways and Off-Gas Stream Characteristics for Aqueous Reprocessing Plants – A Literature Survey and Assessment;* INL/EXT-13-30119; Idaho National Lab. (INL), Idaho Falls, ID (United States), 2013. https://doi.org/10.2172/1111056.

(11) Jubin, R. T.; Jordan, J. A.; Bruffey, S. A. *Extended Elemental Iodine Adsorption by AgZ under Prototypical Vessel Off-Gas Conditions*; ORNL/SPR--2018/884, NTRD-MRWFD--2018-000211, 1470865; 2018; p ORNL/SPR--2018/884, NTRD-MRWFD--2018-000211, 1470865. https://doi.org/10.2172/1470865.

(12) Riley, B.; Soelberg, N.; Jubin, R. T.; Bruffey, S. H.; Strachan, D. M. *Milestone Report - M3FT-15OR03120213 - A Literature Survey to Identify Potentially Problematic Volatile Iodine-Bearing Species Present in Off-Gas Streams*; ORNL/SPR-2015/290; Oak Ridge National Lab. (ORNL), Oak Ridge, TN (United States), **2015**. https://doi.org/10.2172/1393819.

(13) Riley, B. J.; Vienna, J. D.; Strachan, D. M.; McCloy, J. S.; Jerden, J. L. Materials and Processes for the Effective Capture and Immobilization of Radioiodine: A Review. *J. Nucl. Mater.* **2016**, *470*, 307–326. https://doi.org/10.1016/j.jnucmat.2015.11.038.

(14) Aleksandrov, A. B.; Ampelogova, N. I.; Kritskii, V. G.; Krupennikova, V. I.; Kudryashov, L. A.; Petrik, N. G.; Kozlov, E. P.; Kovalev, S. M. Sorption of Molecular Iodine and Methyl Iodide from Air. *Russ. J. Appl. Chem.* **2000**, *73*, 1907–1911.

(15) Stanford, J. P.; van Rooyen, N.; Vaidya, T.; Raja, K. S.; Sabharwall, P.; Utgikar, V. Photodecomposition of Methyl Iodide as Pretreatment for Adsorption of Radioiodine Species in Used Nuclear Fuel Recycling Operations. *Chem. Eng. J.* **2020**, *400*, 125730. https://doi.org/10.1016/j.cej.2020.125730.

(16) Bessonov, A. A.; Kulyukhin, S. A.; Mizina, L. V.; Rumer, I. A. A Study of the Thermal Decomposition of CH3131I in a Gas Flow in the Presence of "Fizkhmin"TM Granulated Materials. *JAMP.* **2016**, *04* (08), 1522–1527. https://doi.org/10.4236/jamp.2016.48161.

(17) Suppes, J. G.; Storvick, S. T, Sustainable Nuclear Power, Chapter 11- Recycling and Waste Handling for Spent Nuclear Fuel. In *Sustain. Nucl. Power*; Elsevier, **2007**, 283–317. https://doi.org/10.1016/B978-012370602-7/50028-4.

(18) Goldstein, L. Electrical Discharge in Gases and Modern Electronics. In Adv. Electron. *Electron Phys. Elsevier,* **1955**, *7*, 399–503. https://doi.org/10.1016/S0065-2539(08)60962-2.

(19) Lister, G. G.; Waymouth, J. F. Light Sources. In Encyclopedia of *Phys. Sci. Int. J.;* Elsevier, **2003**, 557–595. https://doi.org/10.1016/B0-12-227410-5/00378-1.

(20) Andreev, V. V.; Pichugin, Yu. P.; Telegin, V. G.; Telegin, G. G. Study of Electric Discharges between Moving Electrodes in Air. *Plasma Phys. Rep.* **2011**, *37* (12), 1053–1057. https://doi.org/10.1134/S1063780X11110018.

(21) Bisht, S.; Nautiyal, B.; Bhatt, U. M.; Joshi, P. Plasma Applications for Environmental Protection. *Int. J. Eng. Sci. Technol.* 2014, 3 (5), 5.

(22) Laroussi, M. Cold Plasma in Medicine and Healthcare: The New Frontier in Low Temperature Plasma Applications. *Front. Phys.* **2020**, *8* (74). https://doi.org/10.3389/fphy.2020.00074.

(23) Roberts, J. R. 3 - Glow discharges and wall stabilized ARCs. In *Vacuum Ultraviolet Spectroscopy*; Samson, J. A. R., Ederer, D. L., Eds.; Academic Press: Burlington, 2000, 37–63. https://doi.org/10.1016/B978-012617560-8/50004-9.

(24) Xu, X. Dielectric Barrier Discharge — Properties and Applications. *Thin Solid Films.* **2001**, *390* (1–2), 237–242. https://doi.org/10.1016/S0040-6090(01)00956-7.

(25) Kogelschatz, U. Dielectric-Barrier Discharges: Their History, Discharge Physics, and Industrial Applications. *Plasma Chem. Plasma Process.* **2003**, *23*, 1-46.

(26) Kogelschatz, U.; Eliasson, B.; Egli, W. From Ozone Generators to Flat Television Screens: History and Future Potential of Dielectric-Barrier Discharges. *Pure. Appl. Chem.* **1999**, *71* (10), 1819–1828. https://doi.org/10.1351/pac199971101819.

(27) Kebriaei, M.; Ketabi, A.; Halvaei, A. Pulsed Corona Discharge, a New and Effective Technique for Water and Air Treatment. *Biological Forum– An Inter. J.* **2015**, *7*, 1686–1692.

(28) Chen, W.; Chen, X.; Su, X.; Long, Z. Simulation and Analysis of Surface Discharge Development in Oil Immersed Paper Insulation. *Prz. Elektrotech.* **2012**, *88*, 290–295.

(29) Brandenburg, R. Dielectric Barrier Discharges: Progress on Plasma Sources and on the Understanding of Regimes and Single Filaments. *Plasma Sources Sci. Technol.* **2017**, *26* (5), 053001. https://doi.org/10.1088/1361-6595/aa6426.

(30) Gao, G.; Dong, L.; Peng, K.; Wei, W.; Li, C.; Wu, G. Comparison of the Surface Dielectric Barrier Discharge Characteristics under Different Electrode Gaps. *Phys. Plasmas.* **2017**, *24* (1), 013510. https://doi.org/10.1063/1.4974037.

(31) Ju, Y.; Sun, W. Plasma Assisted Combustion: Dynamics and Chemistry. *Prog. Energy Combust. Sci.* **2015**, *48*, 21–83. https://doi.org/10.1016/j.pecs.2014.12.002.

(32) Adamovich, I.; Little, J.; Nishihara, M.; Takashima, K.; Samimy, M. Nanosecond Pulse Surface Discharges for High-Speed Flow Control. In *6th AIAA Flow Control Conference*; American Institute of Aeronautics and Astronautics: New Orleans, Louisiana, 2012. https://doi.org/10.2514/6.2012-3137.

(33) Liu, W.; Wang, Y.; Zhang, H.; Pan, Y.; Dong, L. Note: A Novel Dielectric Barrier Discharge System for Generating Stable Patterns in Wide Range. *Rev. Sci. Instrum.* **2016**, *87* (5), 056101. https://doi.org/10.1063/1.4948735.

(34) Holubová, Ľ.; Kyzek, S.; Ďurovcová, I.; Fabová, J.; Horváthová, E.; Ševčovičová, A.; Gálová, E. Non-Thermal Plasma—A New Green Priming Agent for Plants? *Int. J. Mol. Sci.* **2020**, *21* (24), 9466. https://doi.org/10.3390/ijms21249466.

(35) Misra, N. N.; Yepez, X.; Xu, L.; Keener, K. In-Package Cold Plasma Technologies. *J. Food Eng.* **2019**, *244*, 21–31. https://doi.org/10.1016/j.jfoodeng.2018.09.019.

(36) Bárdos, L.; Baránková, H. Plasma Processes at Atmospheric and Low Pressures. *Vacuum.* **2008**, *83* (3), 522–527. https://doi.org/10.1016/j.vacuum.2008.04.063.

(37) Belasri, A.; Harrache, Z. Electrical and Kinetical Aspects of Homogeneous Dielectric-Barrier Discharge in Xenon for Excimer Lamps. *Phys. Plasmas.* **2010**, *17* (12), 123501. https://doi.org/10.1063/1.3520368.

(38) Wang, Q.; Liu, F.; Miao, C.; Yan, B.; Fang, Z. Investigation on Discharge Characteristics of a Coaxial Dielectric Barrier Discharge Reactor Driven by AC and Ns Power Sources. *Plasma Sci. Technol.* **2018**, *20* (3), 035404. https://doi.org/10.1088/2058-6272/aaa357.

(39) Goldberg, B. M.; Shkurenkov, I.; O'Byrne, S.; Adamovich, I. V.; Lempert, W. R. Electric Field Measurements in a Dielectric Barrier Nanosecond Pulse Discharge with Sub-Nanosecond Time Resolution. *Plasma Sources Sci. Technol.* **2015**, *24* (3), 035010. https://doi.org/10.1088/0963-0252/24/3/035010.

(40) Eriksson, J.; Ulin, J.; Långström, B. [11C]Methyl Iodide from [11C]Methane and Iodine Using a Non-Thermal Plasma Method. *J. Labelled. Compd. Radiopharm.* **2006**, *49* (13), 1177–1186. https://doi.org/10.1002/jlcr.1135.

(41) Steacie, E. W. R.; McDonald, R. D. The Kinetics of the Thermal Decomposition of Gaseous Methyl Iodide. *J. Am. Chem. Soc.* **1935**, *57* (3), 488–488. https://doi.org/10.1021/ja01306a501.

(42) Ogg, R. A. Kinetics of the Thermal Reaction of Gaseous Alkyl Iodides with Hydrogen Iodide. *J. Am. Chem. Soc.* **1934**, *56* (3), 526–536. https://doi.org/10.1021/ja01318a007.

(43) Mikheev, P. A.; Shepelenko, A. A.; Kupryaev, N. V. Production of Atomic Iodine by Decomposition of Methyl Iodide by the Products of a Glow Discharge Plasma in a Flow of Oxygen. *High. Temp.* **2002**, *40* (1), 34-38.

(44) Kalinin, N. N.; Kolyadin, A. B.; Metalidi, M. M.; Vyatkin, V. E. Decomposition of Radioactive Methyl Iodide in an Electric Discharge Field. *Radiochemistry.* **2011**, *53* (2), 202–205. https://doi.org/10.1134/S1066362211020159.

(45) Holm, T. Kinetic Isotope Effects in the Reduction of Methyl Iodide. *J. Am. Chem. Soc.* 1999, *121* (3), 515–518. https://doi.org/10.1021/ja981968.

(46) Ling, S. J.; Sanny, J.; Moebs, W.; Janzen, D. *Introduction to Electricity, Magnetism, and Circuits, 1.4 Electric Field*; University of Saskatchewan, Distance Education Unit, 2018.

(47) Ling, S. J.; Sanny, J.; Moebs, W.; Janzen, D. *Introduction to Electricity, Magnetism, and Circuits, 1.5 Calculating Electric Fields of Charge Distributions*; University of Saskatchewan, Distance Education Unit, 2018.

(48) Ahn, S. K.; Chang, H. Y. Experimental Observation of the Inductive Electric Field and Related Plasma Nonuniformity in High Frequency Capacitive Discharge. *Appl. Phys. Lett.* **2008**, *93* (3), 031506. https://doi.org/10.1063/1.2965118.

(49) Bonaventura, Z.; Bourdon, A.; Celestin, S.; Pasko, V. P. Electric Field Determination in Streamer Discharges in Air at Atmospheric Pressure. *Plasma Sources Sci. Technol.* **2011**, *20* (3), 035012. https://doi.org/10.1088/0963-0252/20/3/035012.